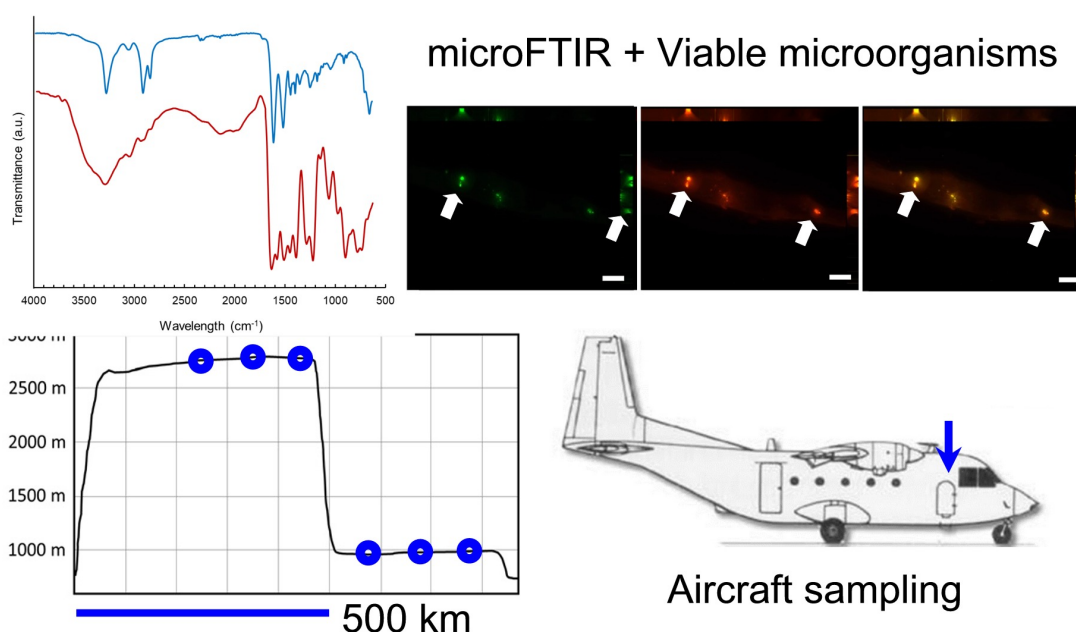


Viabile microorganismi on fibers collected within and beyond the planetary boundary layer

*This manuscript version is made available in fulfillment of publisher's policy.
Please, cite as follows:*

Miguel González-Pleiter, Carlos Edo, María Cristina Casero-Chamorro, Ángeles Aguilera, Elena González-Toril, Jacek Wierzchos, Francisco Leganés, Francisca Fernández-Piñas, and Roberto Rosal. *Viabile Microorganisms on Fibers Collected within and beyond the Planetary Boundary Layer.* *Environmental Science & Technology Letters* Article 7, 11, 819-825, 2020

<https://doi.org/10.1021/acs.estlett.0c00667>



Viable microorganisms on fibers collected within and beyond the planetary boundary layer

Miguel González-Pleiter^{1,3}, Carlos Edo¹, María Cristina Casero-Chamorro¹,
Ángeles Aguilera⁴, Elena González-Toril⁴, Jacek Wierzchos²
Francisco Leganés³, Francisca Fernández-Piñas^{3,*}, and Roberto Rosal^{1,*}

¹Departamento de Ingeniería Química, Universidad de Alcalá, E-28871, Alcalá de Henares, Madrid, Spain

²Departamento de Biogeoquímica y Ecología Microbiana. Museo Nacional de Ciencias Naturales. CSIC. 28006. Madrid. Spain

³Departamento de Biología, Universidad Autónoma de Madrid, Cantoblanco, E-28049 Madrid, Spain

⁴Centro de Astrobiología, CAB (INTA-CSIC), Torrejón de Ardoz, Spain

Abstract

Fibers are found in all environments. However, the impact of their presence on ecosystems and human health is not yet well understood, especially in the case of the atmosphere. In this work, we presented evidence that fibers traveling through the atmosphere act as vectors to spread microorganisms. Here, we investigated the presence of viable microorganisms on fibers collected within and beyond the planetary boundary layer during flights of a C-212 aircraft over Central Spain. In total, seven fibers, six of which transported viable microorganisms, were isolated in two flights. The viability of the microorganisms was determined by confocal microscopy by means of the fluorescent probes SYBR-Green to detect microorganisms and CTC redox dye to assess their cellular respiration activity. The fibers that transported viable microorganisms were spectroscopically analyzed by micro-FTIR and identified as wool-silk and cellulose-cotton. Taken together, the results demonstrated that fibers host viable microorganisms when traveling through the lower free troposphere.

1. Introduction

Airborne particulate matter (APM) may include a biological fraction consisting of bacteria, fungi and other organisms that travel along with natural or anthropogenic particles¹. The transport of bioaerosols may play an important role in the dispersion of microbial populations facilitating their colonization of new habitats or in the spreading of pathogenic strains^{2,3}. The biological material carried by non-biological particles can remain suspended for periods that depend on particle size and are transported by winds, thereby allowing microorganisms to disseminate over long distances. The long-range transport of atmospheric microbiota was suggested by Iwasaka et al., who detected DNA in dust particles collected at 2 km above sea level (a.s.l.) using balloons flying above desertic regions by means of DAPI (4',6-diamidino-2-phenylindole), a DNA-specific probe⁴. The distribution of biological communities in the atmosphere is poorly known as very few investigations exist about airborne microorganisms and high altitudes. Maki et al. showed that the bacterial communities in APM change depending on the origin or air masses. 16S

rDNA sequencing showed that the bacterial communities collected during dust events consisted of sand or terrestrial naturally occurring bacteria in agreement with the continental origin of such air masses⁵. The data available from the pyrosequencing analysis of samples taken from aircrafts flying over the Sea of Japan, indicated that composition changes with consistent with their different origin. Samples at high altitude were dominated by terrestrial bacteria, possibly travelling from continental areas, while samples at lower altitude displayed marine microorganisms and some possibly pathogenic strains⁶.

The concern about anthropogenic environmental pollutants includes fibers, which have been found in essentially all compartments. Some reports evidence the presence of anthropogenic fibers in remote areas, including polar regions proving that atmospheric transport plays an important role in worldwide pollution spreading^{7,8}. Allen et al. reported the presence of fibers in a remote Pyrenean mountain location, interpreted as evidence of long-range transport from populated areas⁹. In the air of urban areas, man-made fibers have also been documented¹⁰. Overall, little is known how these fibers transport through the atmosphere to downwind places that can influence ecosystem and human health. In this work, we presented the first direct evidence that fibers traveling through the atmosphere host viable microorganisms and, therefore, can act as vector for microbial transport between distant places. We investigated

* Corresponding authors: francisca.pina@uam.es, roberto.rosal@uah.es

Available online: August 25, 2020

the presence of viable microorganisms on fibers collected between 300 and 2300 meters above ground level (a.g.l.) using aircrafts from the Spanish National Institute for Aerospace Technology.

2. Materials and methods

Samples taken at 300 and 2300 m a.g.l. were obtained onboard a CASA C-212 turboprop-powered cargo aircraft from the Spanish National Institute of Aerospace Technology (Fig. S1, Supplementary Information, SI). Two flights were performed in Autumn 2019 in Central Spain. One of them above rural areas (Fig. S2, SI) and the other essentially flying over urban zones (Guadalajara, 260 000 inhab., Fig. S3, SI). Both flights took place from 9.00 to 13.00 UTC. The weather was relatively humid, with precipitations 14 mm and 5 mm recorded during the 72 h before each flight (rural and urban respectively). Incoming air was filtered using 25 μm steel meshes fitted inside filter holders directly connected to air intake openings. We used 25 μm mesh because lower openings would result in too low flow of air and because smaller materials cannot be identified by current micro-FTIR apparatus. The location of air sampling lines (Fig. S1, SI) avoided the potential collection of debris produced by the engines, propeller, spinner, and aircraft fairing. Filter holders were sealed after sampling and stored at 4 °C before being opened in sterile conditions. Airflow through filters was measured using a SKC393 flowmeter (SKC, USA). The total volume of air filtered was 12379 L: 3234 L above rural area at 300 m a.g.l., 3373 L above rural area at 2300 m a.g.l., 2769 L above urban area at 300 m a.g.l. and 3003 L above urban area at 2300 m a.g.l. Additional details on sampling procedure can be found elsewhere¹¹. The procedure for preventing contamination is described in SI together with operational details on micro-FTIR analysis.

The viable microorganisms attached to fibers were studied after opening filter holders in sterile conditions and placing steel meshes into clean and sterilized glass Petri dishes that were immediately closed. To avoid contamination, only one fiber per mesh was selected for viability studies using the cell-permeable 5-cyano-2,3-ditoyl tetrazolium chloride (CTC) redox dye. CTC is transformed by actively respiring cells into the fluorescent CTC-formazan, visualized as red fluorescent spots (Ex. 488 nm, Em. 630 nm). SYBR-Green (Invitrogen) was also used for the specific staining of cell nucleic acids (Ex. 488 nm, Em. 510 nm). Epifluorescence images were taken using a Zeiss AxioImager M2 microscope (Carl Zeiss, Germany). Details on staining procedures can be found elsewhere¹².

3. Results and discussion

The planetary boundary layer (PBL) is the turbulent layer of the atmosphere closest to the Earth's surface. PBL height (PBLH) is the altitude over the ground that separates the free troposphere from the turbulent PBL and is an important parameter for pollutant dispersion and air quality modelling¹³. Estimating PBLH is a complex task because of its local and temporal variability, but, overall, PBLH is characterized by a daily cycle with maximum about noontime¹⁴. The average PBLH estimated in the Iberian Peninsula is generally below 2 km a.g.l., coincident with the maximum PBLH recorded in the south of Iberian Peninsula¹⁵. Sicard et al. that PBLH does not change too much along the year, with an average PBLH of 1.45 km within a range from 0.79 to 1.6 km for the north-eastern of the Peninsula¹⁶. Our flight sampled a volume of 6607 L of air above PBHL and 6003 L of air inside PBL. We used 24 filters in two flights (12 per flight). From the total number of filters, 7 of them bore at least one fiber. The total number of fibers was 12 and 3 filters presented more than one fiber and even in this case, only one was taken for viability studies to reduce manipulation. Procedural blanks showed to fibers. One purple fiber (cotton > 80 %) and one red fiber (possibly cotton but with matching < 60 %). No red or purple fibres were found in samples and, therefore, we concluded that no contamination took place. The rest of procedural and cleaning controls did not show any evidence of contamination. The procedure resulted in six fibers bearing viable microorganisms: two fibers collected at 300 m a.g.l. in the urban flight, two fibers collected at 300 m a.g.l. over rural areas, and two more at 2300 m a.g.l. flying over rural areas. Width and length of all fibers are given in Table S1 (SI). The chemical nature of fibers is discussed below.

FTIR spectroscopy was used to assess the chemical composition of fibers. The seven fibers were analysed by micro-FTIR with positive identification (matching ~ 60 % and adequate band assignment for 4 of them). FTIR spectroscopy is a very useful technique for the identification of microplastics. However, obtaining clear spectra from small, and often outside the plane fibers is not an easy task¹⁷. Another difficulty, which is a consequence of the small diameter of some fibers, is the diffraction limit of IR, which is about 10 μm at 1000 cm^{-1} and makes it generally unfeasible obtaining clear spectra of fibers with diameters close to that limit¹⁸. The interference with immersion oil used for bright field and fluorescence microscopy was another difficulty found in this study.

FTIR identification showed the presence of one fiber identified as wool (Fiber #1, 300 m a.g.l.) and

three cellulose-cotton fibers (Fiber #3 at 2300 m a.g.l., and Fibers #4 and #5 at 300 m a.g.l.). Fig. 1 shows the spectra of Fiber #1 (Fig. 1A) and the three cellulose-cotton fibers (Fibers #3, #4 and #5, Fig. 1B) together with their respective standards. All these fibers except Fiber #4 carried viable microorganisms as explained below. The identification of Fiber #1 had some complexity. Based on the wide band at $3000\text{--}3500\text{ cm}^{-1}$, attributed to the stretching vibration of N–H and O–H, the fiber is probably of natural origin as this absorption, broader for natural products, generally allows differentiating wool or silk from synthetic polyamide. However, the hydroxyl band is rather variable from sample to sample as it depends on the amount of adsorbed water. Although the absence of clear scales on the surface of Fiber #1 (Fig. S4A) would be consistent with a synthetic fiber, the overall spectrum matched better with natural wool. Silk is usually identified because of a sharp maximum near 1710 cm^{-1} , which is absent from the spectrum of Fiber #1. The bands typically associated to proteins were also clearly observed. The amide I band due to C=O stretching vibration appears at about 1640 cm^{-1} and the amide II band due to N–H bending and C–N stretching appeared at about 1520 cm^{-1} ¹⁹. Other bands typical from natural wool and similar materials are the C–N stretching (amide III) band at 1380 cm^{-1} and the C–O stretch at 1230 cm^{-1} , all of them clearly identifiable in Fig 1B²⁰.

The FTIR spectra of Fibers #3, #4, and #5 displayed a broad absorption at 3330 cm^{-1} due to the stretching vibration of the hydroxyl group of polysaccharides. The band at 2890 cm^{-1} corresponded to the stretching vibration of C–H bonds in the hydrocarbon constituents of the macromolecule. The peak located at 1640 cm^{-1} was due to absorbed water molecules²¹. The absorption bands at 1425 , 1334 , and 1028 cm^{-1} were attributed to the stretching and bending vibrations of $-\text{CH}_2$ and $-\text{CH}$, $-\text{OH}$ and C–O bonds in cellulose. The absorption band at 894 cm^{-1} is characteristic of the glycosidic bond²².

The presence of microorganisms attached to fibers has been previously reported in several environments such as oceans and sediments^{23–25}. However, little is known about the atmospheric compartment. Direct cell counts allowed the observation and quantification of low biomass samples, i.e.: $\leq 10^2\text{--}10^4$ cells, exploring their presence and metabolic status²⁶. The use of two fluorochromes SYBR-Green and CTC allowed simultaneous assessment of cells attached to the fibers and their metabolic activity. Fig. 2 shows fluorescence microscopy images (SYBR-Green and CTC) of all of them (their characteristics indicated in Table S1). Fig. S5 (SI) shows the only fiber examined (cellulose-cotton) with no cells attached. Cells

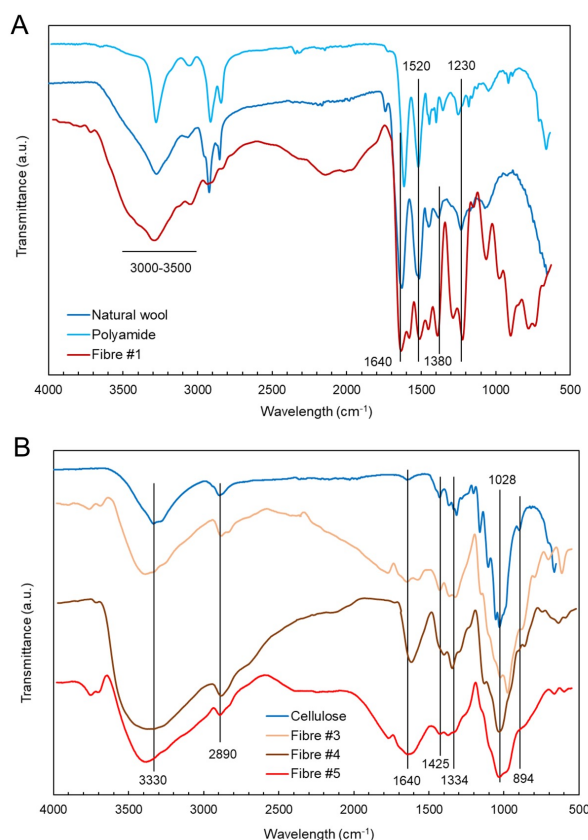


Figure 1: Micro-FTIR spectra of Fiber #1 (identified as wool, A) and Fibers #3, #4 and #5 (identified as cellulose-cotton, B).

showing green fluorescence (SYBR-Green+) (Fig. 2, column A) could be defined as attached, while those simultaneously presenting bright orange CTF fluorescence (SYBR-Green+/CTC+) (Fig. 2, column C) were metabolically active cells. Six fibers collected during both flights exhibited microorganisms attached to their surface. Fluorescence images showed microorganisms scattered along the whole fiber without forming aggregates or colonies, the apparently lack of physical connection between cells suggesting a role of the fiber as physical carrier rather than a substrate colonized by a microbial community. This might imply that microorganisms might have become attached while in the atmosphere; this aspect merits further research.

To check the adequacy of the method to stain attached microorganisms and not nuclei of some biological particles, the same staining procedure used for fibers was applied to fragments of a tree bark, plant leaf hairs, and fungal hyphae. The results are shown in Fig. S6 (SI). Overall, the nuclei inside the cells and the DNA of surface bacteria (only detected on tree bark) showed fluorescence. Specifically, the tree bark did not show any fluorescence, probably because the incubation time was insufficient for the dye to enter cells. However, bacteria were detected

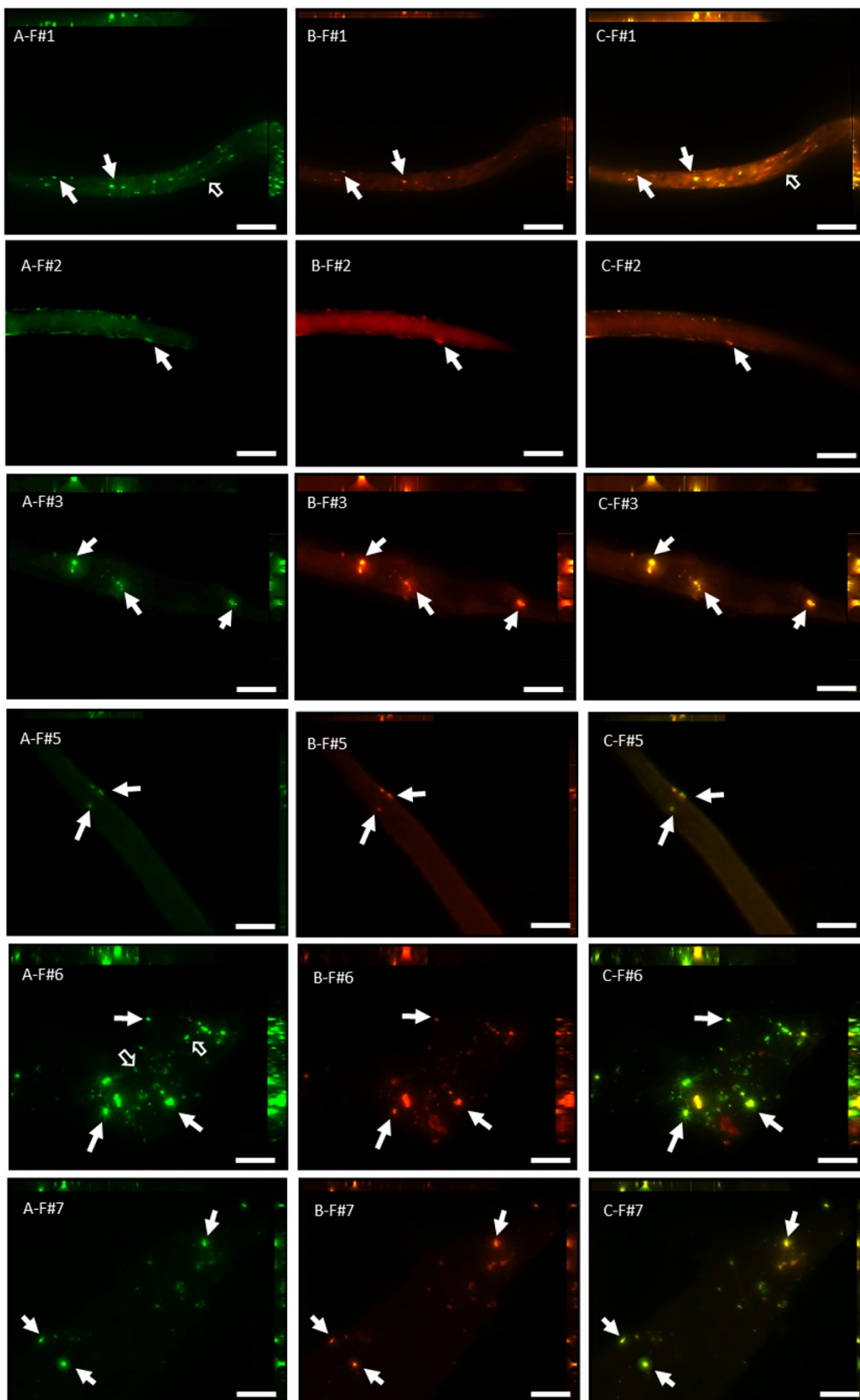


Figure 2: Fluorescence microscopy images showing microorganisms attached to Fibers #1, #2, #3, #5, #6 and #7 (using the same numbers as in Table S1). A-column: Fluorescence image with EGFP filter exhibiting attached cells (SYBR-Green+); B-column: Fluorescence image with HE rhodamine filter showing active cells as revealed by CTC fluorescence (CTC+); C-column: Overlay of EGFP and HE rhodamine filters. Bright dots appearing simultaneously in A and B series indicate attached active cells. Yellow dots in C series indicate presence of both DNA and active cells. White arrows point to attached active cells. Scale bar = 10 μm .

on its surface (Figure S6 A2). In the case of plant leaf hairs, fluorescence micrographs with EGFP filter did not show any attached cells after SYBR-Green staining (Figure S6 B2). The nuclei of fungal cells were clearly stained by SYBR-Green (Figure S6 C2).

Fluorescence microscopy allowed approximate cell counting to estimate the total number of cells harbored by each fiber. Cell counts revealed that each fiber contained between 25 and 50 cells, approx. 70% of which showed metabolic activity. This ratio of metabolic activity, exceeds that observed in other environmental samples studied with the same probe such as sea water (40%)²⁷, coastal sediments (25%)²⁸, temperate lakes (12-20%)²⁹ and sewage activated sludge (55%)³⁰. The surface of the fibers collected in this work ranged between 8×10^3 and $27 \times 10^3 \mu\text{m}^2$ (average $24 \times 10^3 \mu\text{m}^2$), representing about 10^3 metabolically active cells per mm^2 or, converted into mass units, 250 cells/ μg . This is at least one order of magnitude higher than the concentration of viable bacteria observed in dust, but similar to bacterial load on leaves and other plant surfaces, which are in the order of 10^2 cells/ μg ^{31,32}. Expressed in the usual volumetric units, the concentration of fibers measured in this work yielded 0.97 fibers/ m^3 (or 0.68 colonized fibers/ m^3) or 3.0 cells/ m^3 (2 active cells/ m^3). This is below the abundance of bacteria found on moving dust particles, which is in the 10^4 - 10^5 cells/ m^3 range³³. However, this result must be put in the context of the relative abundance of fibers in the atmosphere. Dris et al. reported concentrations of man-made microfibers in urban areas in the 0.3-1.5 fibers/ m^3 range, essentially the same value found in this work¹⁰. The same authors measured concentrations of fibers above 50 μm in indoor and outdoor air with median values of 5.4 and 0.9 fibers/ m^3 respectively³⁴. The number of fibers recovered in our samples was about one fibre per cubic meter, which is compatible with the values reported before.

Up to our knowledge this is the first study reporting the presence of viable microorganisms in fibers collected from the atmosphere. Although it is well known that inter-continentially air transported particles can transport bacteria to distant regions, whether microbes are active in the atmosphere or not is still an area of intense research³⁵. Previous studies in aerobiology introduced the atmosphere as an ecosystem, but in situ reliable measurements of metabolic microbial activity in the atmosphere are scarce³⁶⁻³⁸. The role of natural fibres and textiles as environmental stressors is a topic that has received limited attention in contrast to synthetic or plastics fibers mainly because their biodegradability limits the perception of their risks. Concerning natural materials, biological aerosols are known to play a significant role in atmo-

spheric chemistry. APM includes biological aerosol particles, mostly with rod-like aspect, which are a probable carrier of bacterial and fungal particles³⁹.

We are aware of the limited number of fibers collected in this work. APM is in the atmosphere at low concentration and the capacity of filtering a high volume of air using in situ sampling devices is limited. Future research is needed on the atmospheric lifetime of microorganisms in the atmosphere to evaluate their resistance to stress factors like dryness, low temperature and solar irradiation, which may govern the efficiency of APM for microbial spreading. Another important aspect is to clarify whether the fibers act as physical carrier of microorganisms that have become attached while in the atmosphere or are a substrate colonized in the ground. More research is needed on this topic as studies on the viability of airborne microbial communities are scarce. Culture experiments would be needed to demonstrate the capacity of microorganisms to form colonies or induce infections.

Supporting information

Detailed information about the procedure for preventing contamination and the spectroscopic identification of fibres, details on Aircraft sampling lines, flight altitudes and times, photographs of fibres, bright field and fluorescence micrograph of a non-colonized fiber and micrographs of other materials shown for comparison.

Acknowledgements

The authors acknowledge the financial support provided by the Spanish Government (CTM2016-74927-C2-1-R/2-R, CGL2017-92086-EXP, PGC2018-094076-B-I00, and RTI2018-094867-B-I00). CE thanks the Spanish Ministry of Science, Innovation and Universities for the award of a pre-doctoral grant (FPI). C212 airborne access was generously provided by INTA, coordinated by the Aerial Platform for Research team and with the logistic and operational support of Group 47 of the Spanish Air Force.

References

1. Gat, D.; Mazar, Y.; Cytryn, E.; Rudich, Y., Origin-dependent variations in the atmospheric microbiome community in eastern Mediterranean dust storms. *Environ. Sci. Technol.* 2017, 51, 6709-6718.
2. Maki, T.; Susuki, S.; Kobayashi, F.; Kakikawa, M.; Yamada, M.; Higashi, T.; Chen, B.; Shi, G.; Hong, C.; Tobo, Y.; Hasegawa, H.; Ueda, K.; Iwasaka, Y., Phylogenetic diversity and vertical

- distribution of a halobacterial community in the atmosphere of an Asian dust (KOSA) source region, Dunhuang City. *Air Qual., Atmos. Health* 2008, 1, 81-89.
3. Jaenicke, R., Abundance of cellular material and proteins in the atmosphere. *Science* 2005, 308, 73-73.
 4. Iwasaka, Y.; Shi, G. Y.; Yamada, M.; Kobayashi, F.; Kakikawa, M.; Maki, T.; Naganuma, T.; Chen, B.; Tobo, Y.; Hong, C. S., Mixture of Kosa (Asian dust) and bioaerosols detected in the atmosphere over the Kosa particles source regions with balloon-borne measurements: possibility of long-range transport. *Air Qual., Atmos. Health* 2009, 2, 29-38.
 5. Maki, T.; Hara, K.; Iwata, A.; Lee, K. C.; Kawai, K.; Kai, K.; Kobayashi, F.; Pointing, S. B.; Archer, S.; Hasegawa, H.; Iwasaka, Y., Variations in airborne bacterial communities at high altitudes over the Noto Peninsula (Japan) in response to Asian dust events. *Atmos. Chem. Phys.* 2017, 17, 11877-11897.
 6. Maki, T.; Hara, K.; Kobayashi, F.; Kurosaki, Y.; Kakikawa, M.; Matsuki, A.; Chen, B.; Shi, G.; Hasegawa, H.; Iwasaka, Y., Vertical distribution of airborne bacterial communities in an Asian-dust downwind area, Noto Peninsula. *Atmos. Environ.* 2015, 119, 282-293.
 7. Zhang, Y.; Gao, T.; Kang, S.; Sillanpää, M., Importance of atmospheric transport for microplastics deposited in remote areas. *Environ. Pollut.* 2019, 254, 112953.
 8. González-Pleiter, M.; Velázquez, D.; Edo, C.; Carretero, O.; Gago, J.; Barón-Sola, Á.; Hernández, L. E.; Yousef, I.; Quesada, A.; Leganés, F.; Rosal, R.; Fernández-Piñas, F., Fibers spreading worldwide: Microplastics and other anthropogenic litter in an Arctic freshwater lake. *Sci. Total Environ.* 2020, 722, 137904.
 9. Allen, S.; Allen, D.; Phoenix, V. R.; Le Roux, G.; Durántez Jiménez, P.; Simonneau, A.; Binet, S.; Galop, D., Atmospheric transport and deposition of microplastics in a remote mountain catchment. *Nat. Geosci.* 2019, 12, 339-344.
 10. Dris, R.; Gasperi, J.; Saad, M.; Mirande, C.; Tassin, B., Synthetic fibers in atmospheric fallout: A source of microplastics in the environment? *Mar. Pollut. Bull.* 2016, 104, 290-293.
 11. González-Toril, E.; Osuna, S.; Viúdez-Moreiras, D.; Navarro-Cid, I.; Toro, S. D. d.; Sor, S.; Bardera, R.; Puente-Sánchez, F.; de Diego-Castilla, G.; Aguilera, Á., Impacts of Saharan dust intrusions on bacterial communities of the low troposphere. *Sci. Rep.* 2020, 10, 6837.
 12. Tashyreva, D.; Elster, J.; Billi, D., A novel staining protocol for multiparameter assessment of cell heterogeneity in phormidium populations (cyanobacteria) employing fluorescent dyes. *PLoS One* 2013, 8, e55283.
 13. Li, H.; Yang, Y.; Hu, X.-M.; Huang, Z.; Wang, G.; Zhang, B.; Zhang, T., Evaluation of retrieval methods of daytime convective boundary layer height based on lidar data. *J. Geophys. Res.: Atmos.* 2017, 122, 4578-4593.
 14. Banks, R. F.; Tiana-Alsina, J.; Rocadenbosch, F.; Baldasano, J. M., Performance evaluation of the boundary-layer height from lidar and the weather research and forecasting model at an urban coastal site in the North-East Iberian Peninsula. *Boundary-Layer Meteorol.* 2015, 157, 265-292.
 15. de Arruda-Moreira, G.; Guerrero-Rascado, J. L.; Bravo-Aranda, J. A.; Benavent-Oltra, J. A.; Ortiz-Amezcuca, P.; Róman, R.; Bedoya-Velásquez, A. E.; Landulfo, E.; Alados-Arboledas, L., Study of the planetary boundary layer by microwave radiometer, elastic lidar and Doppler lidar estimations in Southern Iberian Peninsula. *Atmos. Res.* 2018, 213, 185.
 16. Sicard, M.; Pérez, C.; Rocadenbosch, F.; Baldasano, J. M.; García-Vizcaino, D., Mixed-layer depth determination in the Barcelona coastal area from regular lidar measurements: Methods, results and limitations. *Boundary-Layer Meteorol.* 2006, 119, 135-157.
 17. Stanton, T.; Johnson, M.; Nathanail, P.; MacNaughtan, W.; Gomes, R. L., Freshwater and airborne textile fibre populations are dominated by 'natural', not microplastic, fibres. *Sci. Total Environ.* 2019, 666, 377-389.
 18. Primpke, S.; Lorenz, C.; Rascher-Friesenhausen, R.; Gerdts, G., An automated approach for microplastics analysis using focal plane array (FPA) FTIR microscopy and image analysis. *Anal. Methods* 2017, 9, 1499-1511.
 19. Peets, P.; Kaupmees, K.; Vahur, S.; Leito, I., Reflectance FT-IR spectroscopy as a viable option for textile fiber identification. *Heritage Sci.* 2019, 7, 93.
 20. McGregor, B. A.; Liu, X.; Wang, X. G., Comparisons of the Fourier Transform Infrared Spectra of cashmere, guard hair, wool and other animal fibres. *J. Text. Inst.* 2018, 109, 813-822.
 21. Poletto, M.; Pistor, V.; Zeni, M.; Zattera, A. J., Crystalline properties and decomposition kinetics of cellulose fibers in wood pulp obtained by two pulping processes. *Polym. Degrad. Stab.* 2011, 96, 679-685.

22. Xu, F.; Yu, J.; Tesso, T.; Dowell, F.; Wang, D., Qualitative and quantitative analysis of ligno-cellulosic biomass using infrared techniques: A mini-review. *Appl. Energy* 2013, 104, 801-809.
23. Kettner, M. T.; Oberbeckmann, S.; Labrenz, M.; Grossart, H.-P., The eukaryotic life on microplastics in brackish ecosystems. *Front. Microbiol.* 2019, 10,
24. Oberbeckmann, S.; Labrenz, M., Marine microbial assemblages on microplastics: Diversity, adaptation, and role in degradation. *Ann. Rev. Mar. Sci.* 2020, 12, 209-232.
25. Khoironi, A.; Hadiyanto, H.; Anggoro, S.; Sudarno, S., Evaluation of polypropylene plastic degradation and microplastic identification in sediments at Tambak Lorok coastal area, Semarang, Indonesia. *Mar. Pollut. Bull.* 2020, 151, 110868.
26. Zhong, Z.-P.; Solonenko, N. E.; Gazitúa, M. C.; Kenny, D. V.; Mosley-Thompson, E.; Rich, V. I.; Van Etten, J. L.; Thompson, L. G.; Sullivan, M. B., Clean low-biomass procedures and their application to ancient ice core microorganisms. *Front. Microbiol.* 2018, 9.
27. Caruso, G.; Caruso, R.; Maimone, G., Microbial enzymatic activity measurements by fluorogenic substrates: Evidence of inducible enzymes in oligotrophic Mediterranean areas. *J. Clin. Microbiol. Biochem. Technol.* 2019, 5, 19-24.
28. Proctor, L. M.; Souza, A. C., Method for enumeration of 5-cyano-2, 3-ditoyl tetrazolium chloride (CTC)-active cells and cell-specific CTC activity of benthic bacteria in riverine, estuarine and coastal sediments. *J. Microbiol. Methods* 2001, 43, 213-222.
29. Søndergaard, M.; Danielsen, M., Active bacteria (CTC+) in temperate lakes: temporal and cross-system variations. *J. Plankton Res.* 2001, 23, 1195-1206.
30. Yoshida, N.; Fujii, Y.; Hiraishi, A., A modified cyanoditoyl tetrazolium reduction method for differential detection of metabolically active gram-positive and gram-negative bacteria. *Microbes Environ.* 2006, 21, 272-277.
31. Jeon, E. M.; Kim, H. J.; Jung, K.; Kim, J. H.; Kim, M. Y.; Kim, Y. P.; Ka, J.-O., Impact of Asian dust events on airborne bacterial community assessed by molecular analyses. *Atmos. Environ.* 2011, 45, 4313-4321.
32. Lindow, S. E.; Brandl, M. T., Microbiology of the Phyllosphere 2003, 69, (4), 1875-1883.
33. Yamaguchi, N.; Ichijo, T.; Sakotani, A.; Baba, T.; Nasu, M., Global dispersion of bacterial cells on Asian dust. *Sci. Rep.* 2012, 2, 525.
34. Dris, R.; Gasperi, J.; Mirande, C.; Mandin, C.; Guerrouache, M.; Langlois, V.; Tassin, B., A first overview of textile fibers, including microplastics, in indoor and outdoor environments. *Environ. Pollut.* 2017, 221, 453-458.
35. Zhai, Y.; Li, X.; Wang, T.; Wang, B.; Li, C.; Zeng, G., A review on airborne microorganisms in particulate matters: Composition, characteristics and influence factors. *Environ. Int.* 2018, 113, 74-90.
36. Diehl, R. H., The airspace is habitat. *Trends Ecol. Evol.* 2013, 28, 377-379.
37. Šantl-Temkiv, T.; Finster, K.; Hansen, B. M.; Pašić, L.; Karlson, U. G., Viable methanotrophic bacteria enriched from air and rain can oxidize methane at cloud-like conditions. *Aerobiologia* 2013, 29, 373-384.
38. Vaitilingom, M.; Deguillaume, L.; Vinatier, V.; Sancelme, M.; Amato, P.; Chaumerliac, N.; Delort, A.-M., Potential impact of microbial activity on the oxidant capacity and organic carbon budget in clouds. *Proc. Natl. Acad. Sci. U.S.A.* 2013, 110, 559-564.
39. Li, W.; Liu, L.; Xu, L.; Zhang, J.; Yuan, Q.; Ding, X.; Hu, W.; Fu, P.; Zhang, D., Overview of primary biological aerosol particles from a Chinese boreal forest: Insight into morphology, size, and mixing state at microscopic scale. *Sci. Total Environ.* 2020, 719, 137520.

Supplementary Information

Viable microorganisms on fibers collected within and beyond the planetary boundary layer

Miguel González-Pleiter^{1,3}, Carlos Edo¹, María Cristina Casero-Chamorro¹,
Ángeles Aguilera⁴, Elena González-Toril⁴, Jacek Wierzchos²
Francisco Leganés³, Francisca Fernández-Piñas^{3,*}, and Roberto Rosal^{1,*}

¹Departamento de Ingeniería Química, Universidad de Alcalá, E-28871, Alcalá de Henares, Madrid, Spain

²Departamento de Biogeoquímica y Ecología Microbiana. Museo Nacional de Ciencias Naturales. CSIC. 28006. Madrid. Spain

³Departamento de Biología, Universidad Autónoma de Madrid, Cantoblanco, E-28049 Madrid, Spain

⁴Centro de Astrobiología, CAB (INTA-CSIC), Torrejón de Ardoz, Spain

* Corresponding authors: francisca.pina@uam.es, roberto.rosal@uah.es

Contents

Materials and Methods

Figure S1. Aircraft CASA C-212 Aviocar with blue arrows indicating air sampling lines. A and B) The scheme shows the six air sampling lines located at the leading edge of the airplane on both sides (left: L1, L2, L3; right: R1, R2 and R3). C) Detail of the air sampling lines located on the left side.

Figure S2. Sampling profile (A; red line) and information (B; altitude above sea level and distance) of the flight above rural areas (Flight 1). Flight 1 started at 9.00 UTC on November 12th, 2019 and ended the same day at 12.30 UTC. (Initial and final altitude 618 m a.s.l.)

Figure S3. Sampling profile (A; red line) and information (B; altitude above sea level and distance) of the flight above urban areas (Flight 2). Flight 2 started at 9.30 UTC on December 3rd, 2019 and ended the same day at 13.30 UTC. (Initial and final altitude 618 m a.s.l.)

Table S1. Characteristics of collected fibers.

Figure S4. Photographs of Fibers #1 (A), #3 (B) #4 (C) and #5 (D). Mesh size opening: 25 μm . FTIR spectra are shown in Fig. 1.

Figure S5. Bright field and fluorescence microscopy of a fiber (cotton-cellulose) collected at 300 m a.g.l. with no microbial cells attached. Series A) Bright field image; Series B) Fluorescence image with EGFP filter set exhibiting no attached cells after SYBR-Green staining. Series C) Fluorescence image with HE rhodamine filter set exhibiting no metabolically active cells after CTC staining. Scale bar = 20 μm

Figure S6. Micrographs showing tree bark (A), plant leaf hair (B) and fungal cells (C) stained with SYBR-Green and CTC. A1, B1 and C1: Bright field images. A2, B2 and C2: Fluorescence images with EGFP filter. A3, B3 and C3: Fluorescence image with HE rhodamine filter. A4, B4, C4: μFTIR representative spectra. Scale bar 10 μm .

Materials and methods

Procedure for preventing contamination. All metal, steel and glass materials were carefully cleaned with Milli-Q water, wrapped with aluminum foil, and heated to 300 °C for 3 h in order to remove all possible rests of organic matter. Steel meshes were also heated at 300 °C for 3 h to remove all possible fibers or particles and carefully fitted inside clean filter holders. Filter holders with filters were individually wrapped with aluminum foil and sterilized at 115 °C. The use of any plastic material was avoided except for the polycarbonate filter holders.

To account for possible contamination associated with sampling and sample processing, negative controls were performed as follows: (i) two procedural controls per flight consisting of 25 µm steel meshes previously heated to 300 °C for 3 h, fitted into their holders and sterilized at 115 °C for 15 min were exposed to during flights except for air filtration; (ii) one blank per flight consisted of a glass Petri dish with one 25 µm steel mesh previously heated to 300 °C for 3 h and kept open during sampling to identify possible contamination inside the aircraft and when fibers were collected and placed in sterile conditions on glass slides; and (iii) all surfaces, including sampling lines, were cleaned with filtered ethanol 70 % (v/v) before each flight. All controls were treated the same way as samples throughout the entire experimental process.

Spectroscopic identification. After analyzing the viable microorganisms attached to sampled fiber, the same fibers were analysed by micro-Fourier Transform Infrared Spectroscopy (µFTIR) using a Perkin-Elmer Spotlight 200 Spectrum Two device with mercury cadmium telluride detector. For FTIR analyses, individual fibers were placed on potassium bromide discs with a zircon microneedle. The equipment operated in micro-transmission mode with the following parameters: spot 50 µm, 32 scans, and spectral range 550-4000 cm⁻¹ with 8 cm⁻¹ resolution. The spectra were processed by means of Omnic software (Thermo Fisher) and compared with Omnic 9 database or with spectra from other samples and standards recorded by our group.

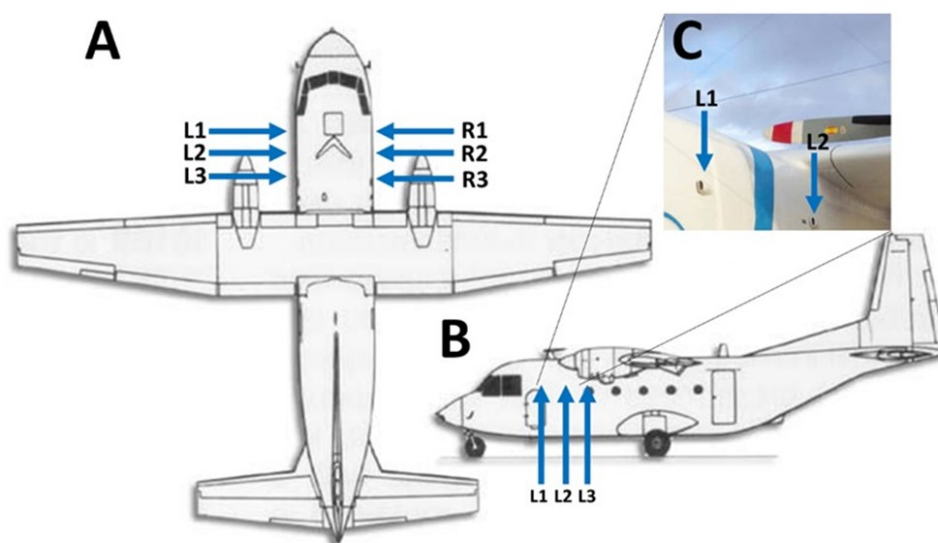
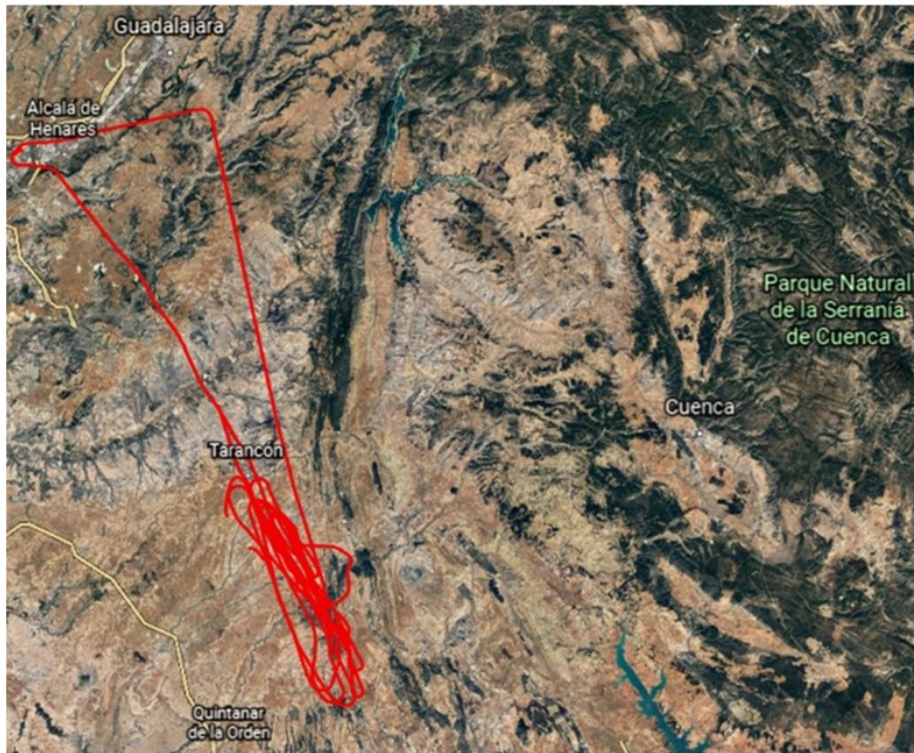


Figure S1: Aircraft CASA C-212 Aviocar with blue arrows indicating air sampling lines. A and B) The scheme shows the six air sampling lines located at the leading edge of the airplane on both sides (left: L1, L2, L3; right: R1, R2 and R3). C) Detail of the air sampling lines located on the left side.

A



B

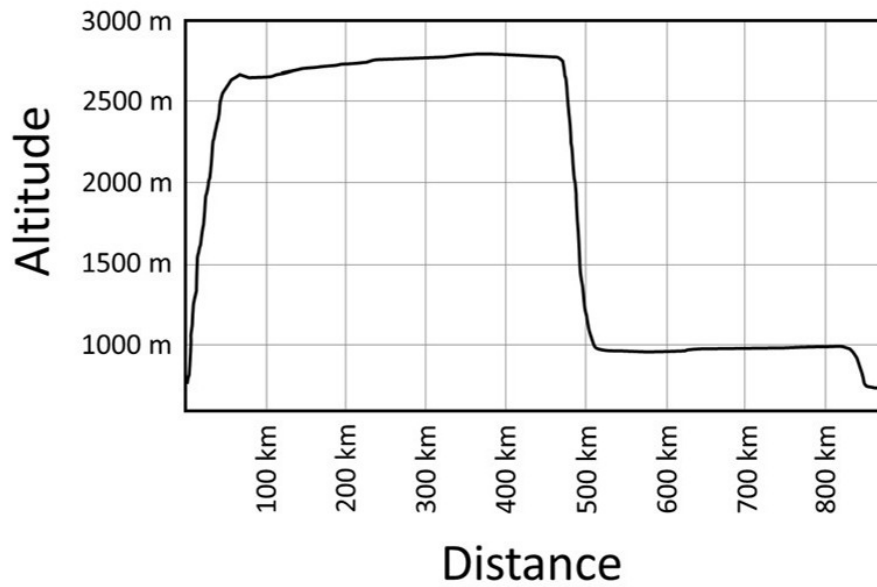
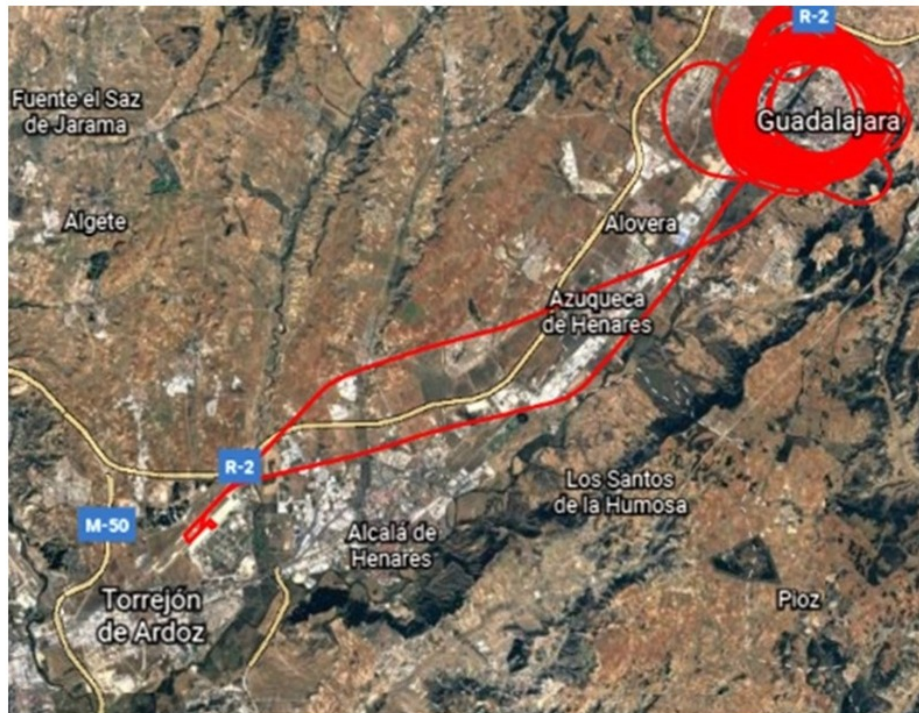


Figure S2: Sampling profile (A; red line) and information (B; altitude above sea level and distance) of the flight above rural areas (Flight 1). Flight 1 started at 9.00 UTC on November 12th, 2019 and ended the same day at 12.30 UTC. (Initial and final altitude 618 m a.s.l.)

A



B

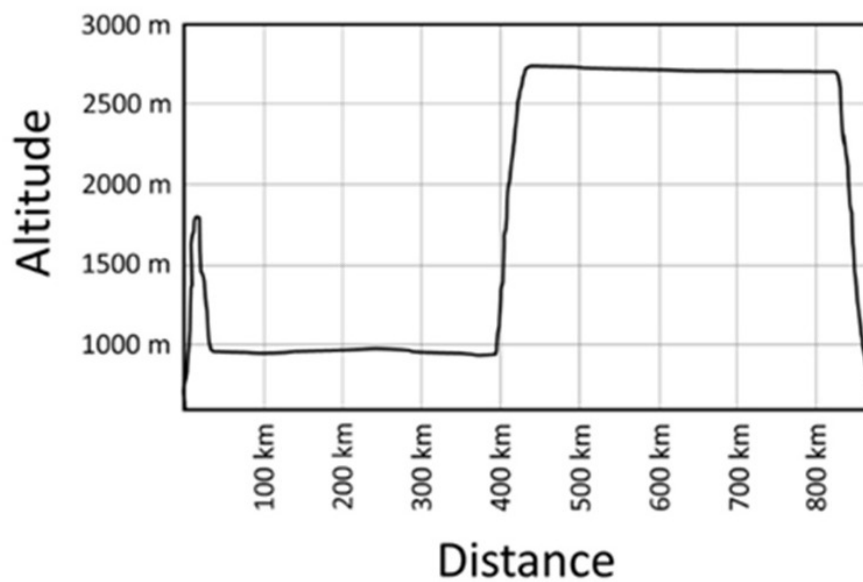


Figure S3: Sampling profile (A; red line) and information (B; altitude above sea level and distance) of the flight above urban areas (Flight 2). Flight 2 started at 9.30 UTC on December 3rd, 2019 and ended the same day at 13.30 UTC. (Initial and final altitude 618 m a.s.l.)

Table S1. Characteristics of collected fibers.

Id.	Height (a.g.l.)	Width (μm)	Length (μm)	Notes on the identification of fibers	Colonized
Fiber #1	300 m	18.4	623	Natural fiber/textile, probably wool	Yes
Fiber #2	300 m	15.3	603	Natural fiber/textile	Yes
Fiber #3	2300 m	16.7	511	Natural fiber/textile (cotton-cellulose)	Yes
Fiber #4	300 m	21.9	393	Natural fiber/textile (cotton-cellulose)	Yes
Fiber #5	2300 m	16.9	452	Natural fiber/textile (cotton-cellulose)	Yes
Fiber #6	300 m	12.8	420	Natural fiber/textile	Yes
Fiber #7	2300 m	9.2	267	Natural fiber/textile	Yes

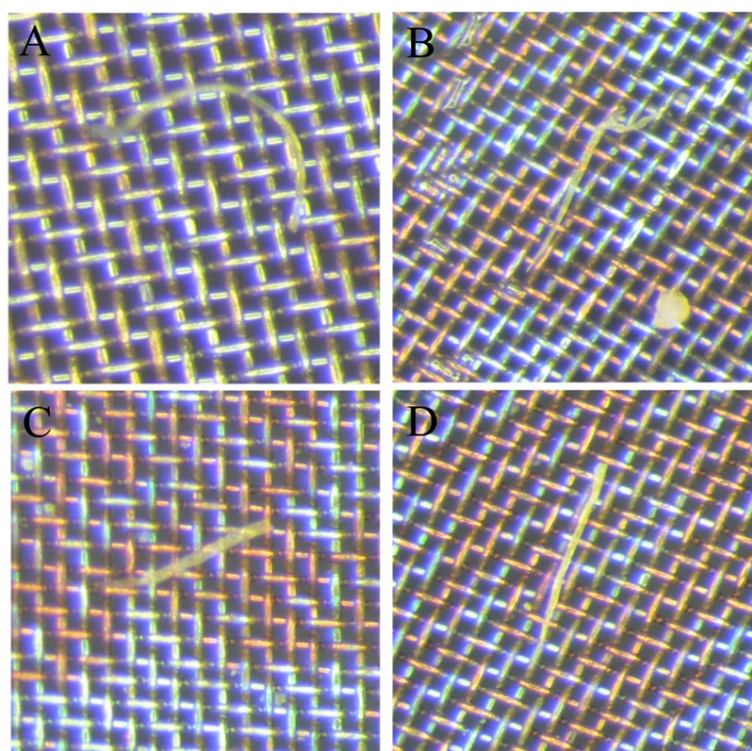


Figure S4: Photographs of Fibers #1 (A), #3 (B) #4 (C) and #5 (D). Mesh size opening: 25 μm . FTIR spectra are shown in Fig. 1.

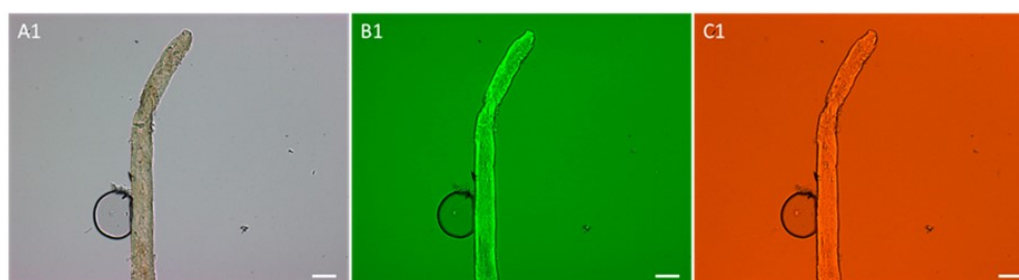


Figure S5: Bright field and fluorescence microscopy of a fiber (cotton-cellulose) collected at 300 m a.g.l. with no microbial cells attached. Series A) Bright field image; Series B) Fluorescence image with EGFP filter set exhibiting no attached cells after SYBR-Green staining. Series C) Fluorescence image with HE rhodamine filter set exhibiting no metabolically active cells after CTC staining. Scale bar = 20 μm .

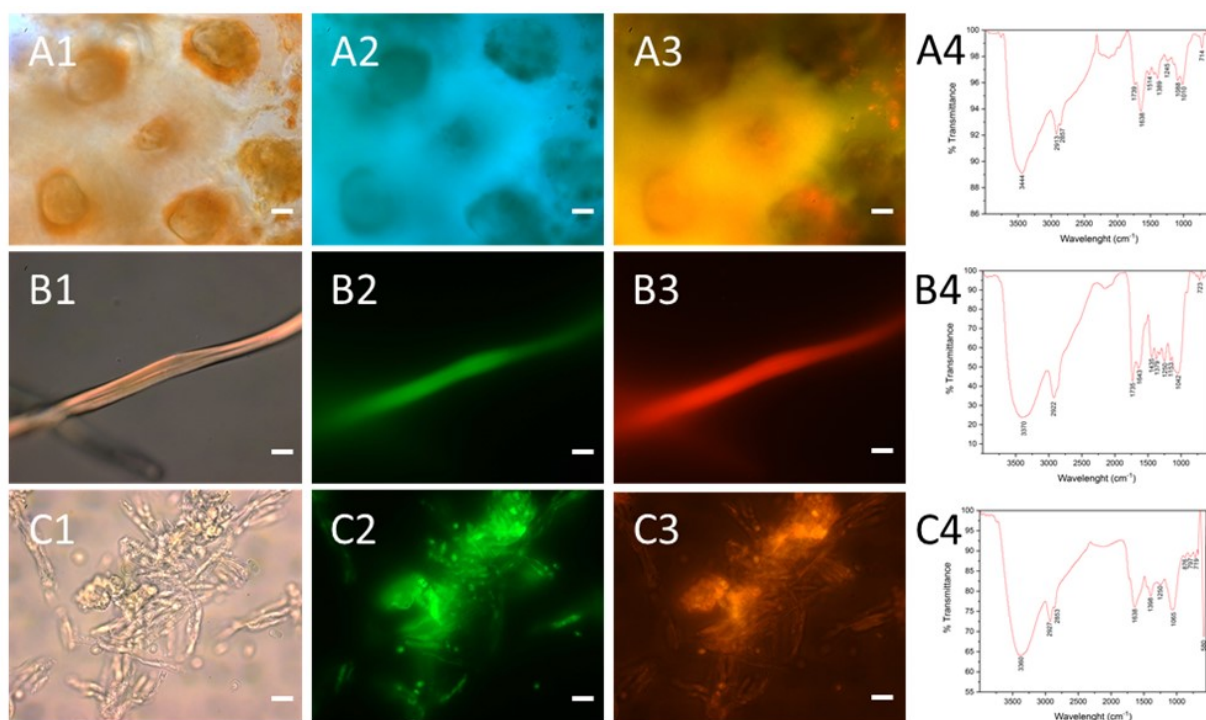


Figure S6: Micrographs showing tree bark (A), plant leaf hair (B) and fungal cells (C) stained with SYBR-Green and CTC. A1, B1 and C1: Bright field images. A2, B2 and C2: Fluorescence images with EGFP filter. A3, B3 and C3: Fluorescence image with HE rhodamine filter. A4, B4, C4: μ FTIR representative spectra. Scale bar 10 μ m.